CHARACTERISTICS IN AN RF SUPERCONDUCTING QUANTUM INTERFERENCE DEVICE AS A FUNCTION OF APPLIED MAGNETIC FLUX : SYSTEMATIC CALCULATIONS II

メタデータ	言語: eng
	出版者: 室蘭工業大学
	公開日: 2014-03-04
	キーワード (Ja):
	キーワード (En):
	作成者: 青地, 強志, 戎, 修二, 永田, 正一
	メールアドレス:
	所属:
URL	http://hdl.handle.net/10258/591

CHARACTERISTICS IN AN RF SUPERCONDUCTING QUANTUM INTERFERENCE DEVICE AS A FUNCTION OF APPLIED MAGNETIC FLUX : SYSTEMATIC CALCULATIONS ?

著者	AOCHI Tsuyoshi, EBISU Shuji, NAGATA Shoichi
journal or publication title	Memoirs of the Muroran Institute of Technology. Science and engineering
volume	42
page range	45-66
year	1992-11
URL	http://hdl.handle.net/10258/591

CHARACTERISTICS IN AN RF SUPERCONDUCTING QUANTUM INTERFERENCE DEVICE AS A FUNCTION OF APPLIED MAGNETIC FLUX : SYSTEMATIC CALCULATIONS II

Tsuyoshi AOCHI, Shuji EBISU and Shoichi NAGATA

Abstract

Characteristic feature in superconducting quantum interference device (*rf* – SQUID) is shown on the basis of the analysis of the foregoing paper. The behavior will be given in detail. The parameter $\beta = (2\pi LI_0) / \Phi_0$ changes gradually the characteristic feature, here I_0 is the critical current of the junction, L is the self – inductance of the ring and Φ_0 is the flux quantum. Abrupt transitions between two adjacent quantum states are clearly shown in the regime $\beta > 1$. The results of the systematic calculations of the characteristics in the *rf* – SQUID are presented over the range of $\beta = 0.20$ to 2π.

1. Introduction

The superconducting quantum interference device (*rf* – SQUID) is based on the two physical pillars. The first is fluxoid quantization and the second is Josephson effect. Figure 1 shows a superconducting ring with a single Josephson weak link. We shall make the simplification that the ideal Josephson junction area is small enough for the current density to be uniform, and that it never contains a significant fraction of a flux quantum. The internal magnetic flux Φ passing through the ring includes the magnetic flux LI_s generated by the current I_s circulating in the ring, where L is the self – inductance of the ring. As shown in Fig. 1, the internal flux Φ threading the ring is then related to the applied flux Φ_x by $\Phi = \Phi_x - LI_s$, where Φ_x is the applied flux intercepted by the ring, and LI_s is the screening flux generated by the induced supercurrent.

In the present paper, many physical quantities have been calculated as a function of applied magnetic flux Φ_x. Their behavior depends on the dimensionless parameter $\beta = (2\pi LI_0) / \Phi_0$, where I_0 is the critical current of the junction and Φ_0 is the flux quantum.

Our numerical calculations have been carried out for values of β from 0.20 to 2π. The present work is concerned with systematic computer calculations of the static behavior of the *rf* – SQUID, which is based on the theoretical investigation given in the previous paper of this volume.[1)] Here we will present further detailed characteristics of the *rf* – SQUID.

2. Basic Equations

The basic equations are summarized and are described below. The main characteristics of the *rf* – SQUID are the behaviors of the internal flux Φ and of the screening circulating current I_s as a function of the external flux Φ_x. They are derived from the next equations,

$$\Phi = \Phi_x - LI_s, \tag{1}$$

$$\theta = 2\pi\ [\Phi / \Phi_0 + n], \tag{2}$$

$$I_s = I_0 \sin\theta . \tag{3}$$

Equations (1), (2) and (3) are linked equations for the three unknown quantities Φ, I_s and θ in terms of the applied flux Φ_x. Here we introduce dimensionless parameter β, defined as

$$\beta = (2\pi LI_0) / \Phi_0, \tag{4}$$

where β depends on the value of LI_0. The limiting forms of the equations are $\Phi = \Phi_x$ for $LI_0 = 0$, which corresponds to an open ring, and complete flux quantization $\Phi = n\Phi_0$ for $LI_0 \gg \Phi_0$, which corresponds to a closed ring with no weak link. Making the substitution of eqs. (2) and (3) into eq. (1), we get a next relation,

$$\Phi = \Phi_x - LI_0 \sin(2\pi\Phi / \Phi_0). \tag{5}$$

Substituting eqs. (1) and (2) into eq. (3) gives

$$I_s = I_0 \sin(2\pi\Phi / \Phi_0). \tag{6}$$

For the ring with a junction the energy of the system is given by

$$U = (\frac{1}{2L})(\Phi - \Phi_x)^2 - E_0 \cos(\frac{2\pi\Phi}{\Phi_0}). \tag{7}$$

3. Numerical Computer Calculations for the Characteristics in *rf* – SQUID

We have investigated the following problems on the basis of the theoretical analysis of the foregoing our paper :[1)]

1. The system energy $U(\Phi, \Phi_x)$
2. The junction coupling energy E_J vs. external flux Φ_x

3. The magnetic energy E_m vs. external flux Φ_x

4. E_J, E_m vs. phase difference θ

5. Internal flux Φ vs. external flux Φ_x

6. Induced flux LI_s vs. external flux Φ_x

7. Phase difference θ vs. external flux Φ_x

8. Fluxoid vs. external flux Φ_x

The results of the systematic calculations are shown in Figs 2 to 35.

4. Summary

Static characteristics of an *rf* – SQUID are described on the basis of numerical computer calculations. Systematic changes in the behavior of a superconducting ring are found when the parameter β varies from 0.20 to 2π.

When $\beta > 1$, the internal flux Φ and the screening current I_s are continuous single valued functions of the external flux Φ_x. There are no sudden transitions, the superconducting ring can go continuously from one quantum state to the next.

For $\beta > 1$, the transitions between two quantum states are irreversible. The transition to successive fluxoid takes place at $\theta = \cos^{-1}(-1/\beta)$. The maximum in the system energy $U(\theta)$ corresponds to the critical external flux Φ_{xc} at which the internal flux Φ and the screening current I_s have an infinite slope as a function of the external flux Φ_x. From the energy view point of $U(\Phi, \Phi_x)$, Φ_{xc} corresponds to the value at which the system changes from metastable state to the stable state.

Acknowledgment

The auther (S. N.) would like to thank Professor M. Ocio for critical reading of these manuscripts.

Reference

1) T. Aochi, S. Ebisu and S. Nagata : Memoirs of the Muroran Institute of Technology (Science and Engineering) 42, (1992) p.33, (preceding paper in this volume).

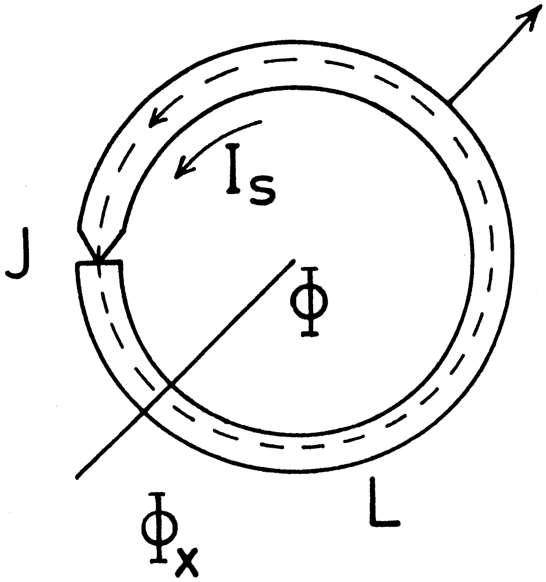

Fig. 1 Superconducting ring with a ideal Josephson junction denoted by J. The contour used for integration is shown by the broken line. Internal magnetic flux Φ, circulating current I_s, self – inductance L and applied magnetic flux Φ_x are related by $\Phi = \Phi_x - LI_s$. Typical values are $L = 5$ nH, and $I_0 = 1\,\mu$A. The junction resistance in the normal state is $R = 10\,\Omega$, and the diameter of the ring is about 2mm.

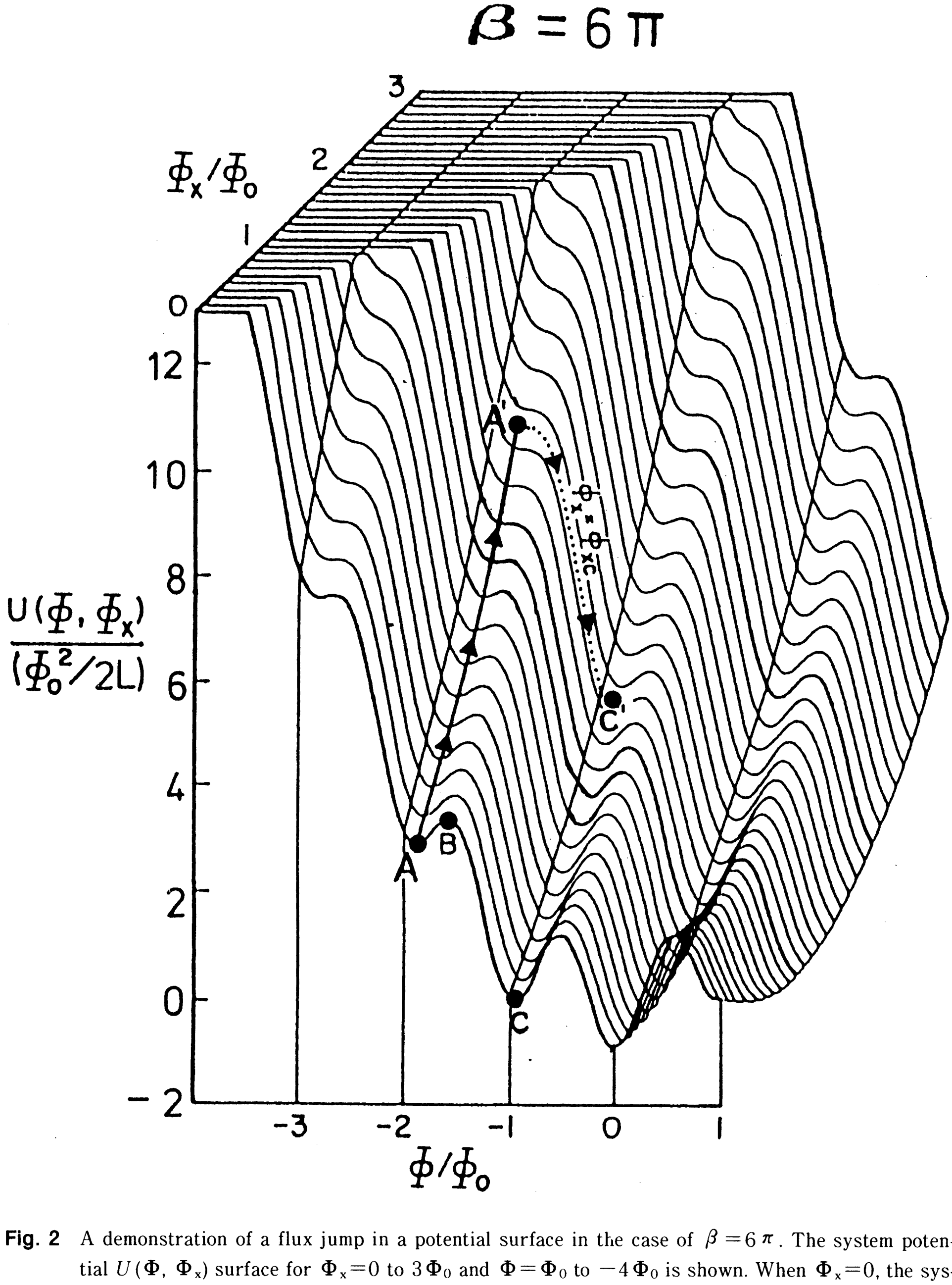

Fig. 2 A demonstration of a flux jump in a potential surface in the case of $\beta = 6\pi$. The system potential $U(\Phi, \Phi_x)$ surface for $\Phi_x = 0$ to $3\Phi_0$ and $\Phi = \Phi_0$ to $-4\Phi_0$ is shown. When $\Phi_x = 0$, the system is trapped around a minimum such as point A in the potential well associated with a fluxoid quantum state. The system is constrained by a potential barrier at B. As Φ_x is increased, the potential energy increases along the valley A — A′ and the system can transfer from point A′, where $\Phi_x = \Phi_{xc}$ and $\Delta U = 0$, to point C′.

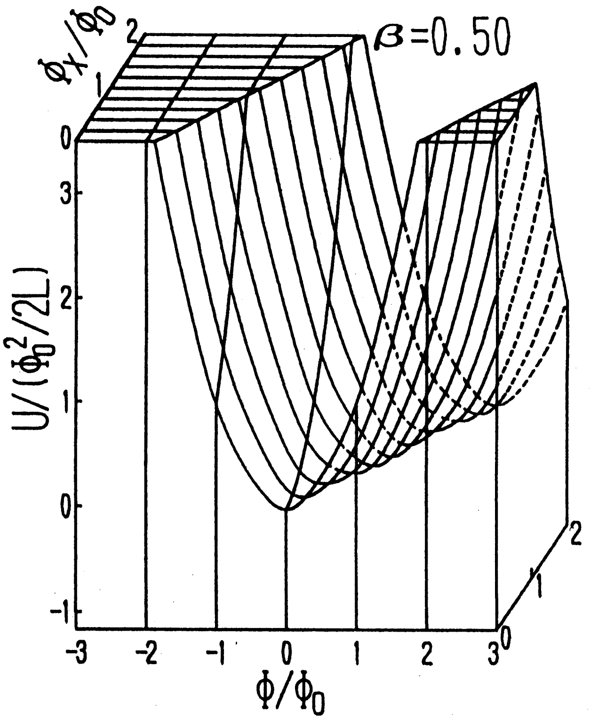

Fig. 3 Potential $U(\Phi, \Phi_x)$ surface for $\Phi_x = 0$ to $2\Phi_0$ and $\Phi = 3\Phi_0$ to $-3\Phi_0$ in the case where $\beta = 0.50$. The sharp transition can not occur between the two adjacent quantum states.

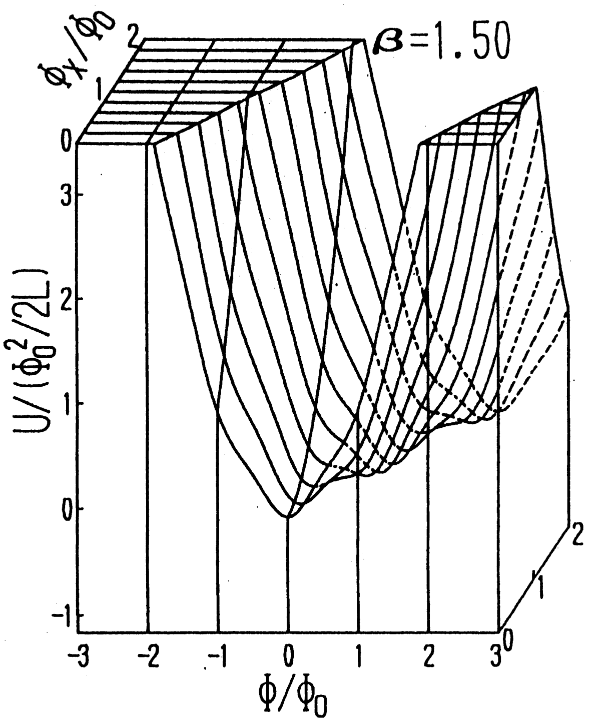

Fig. 4 Potential $U(\Phi, \Phi_x)$ surface for $\Phi_x = 0$ to $2\Phi_0$ and $\Phi = 3\Phi_0$ to $-3\Phi_0$ in the case where $\beta = 1.50$. The sharp transitions can occur between the two adjacent quantum states at $\Phi_x = 0.544\Phi_0$ and $0.456\Phi_0$ in the irreversible process, see Fig. 9.

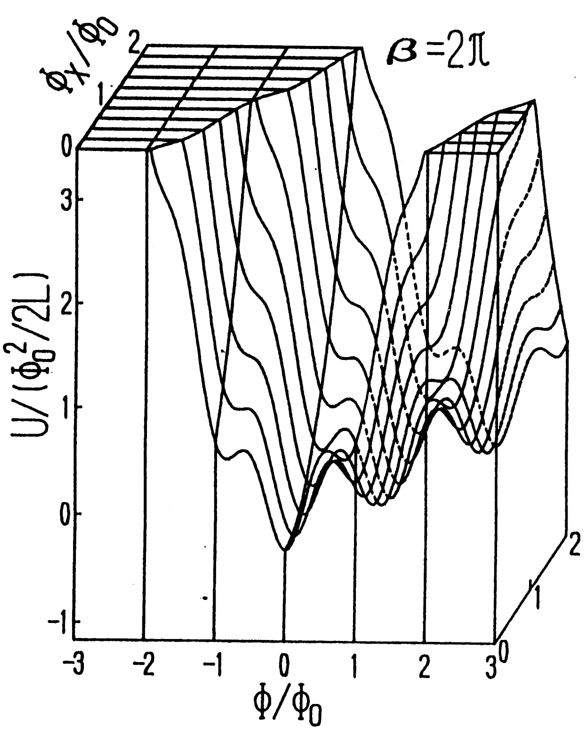

Fig. 5 Potential $U(\Phi, \Phi_x)$ surface for $\Phi_x = 0$ to $2\Phi_0$ and $\Phi = 3\Phi_0$ to $-3\Phi_0$ in the case where $\beta = 2\pi$. The sharp transitions can occur between the two adjacent quantum states, see Fig. 11.

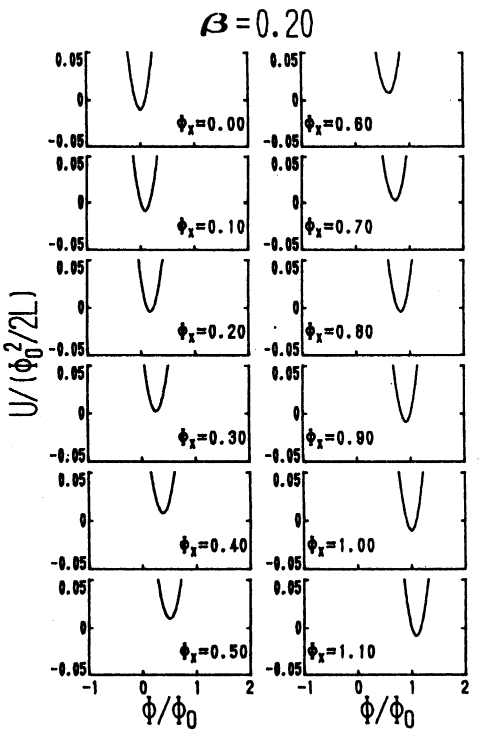

Fig. 6 System energy U for $\beta = 0.20$ as a function of Φ. The energy minimum shifts gradually from a flux quantum state to a neighbor state when the external magnetic flux Φ_x changes. The value of Φ_x denoted in each graph is normalized by Φ_0.

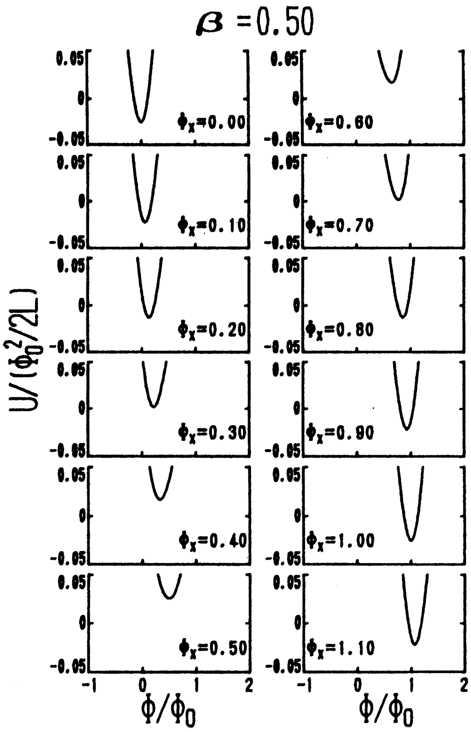

Fig. 7 System energy U for $\beta = 0.50$ as a function of Φ. The value of Φ_x changes from 0.0 to 1.10.

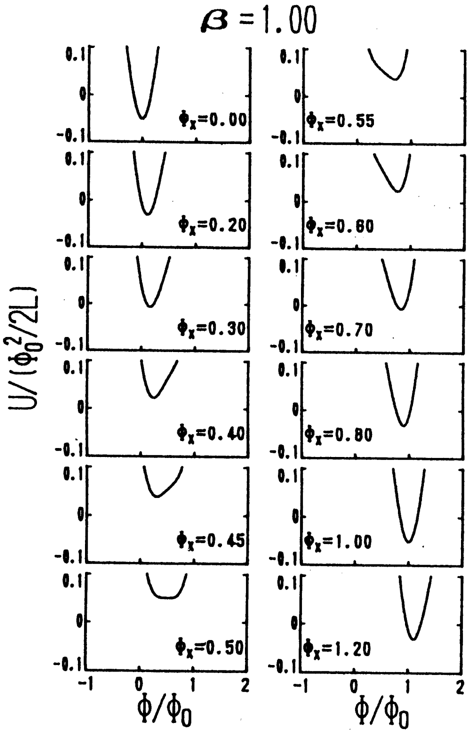

Fig. 8 System energy U for $\beta = 1.00$ as a function of Φ. The value of Φ_x changes from 0.0 to 1.20.

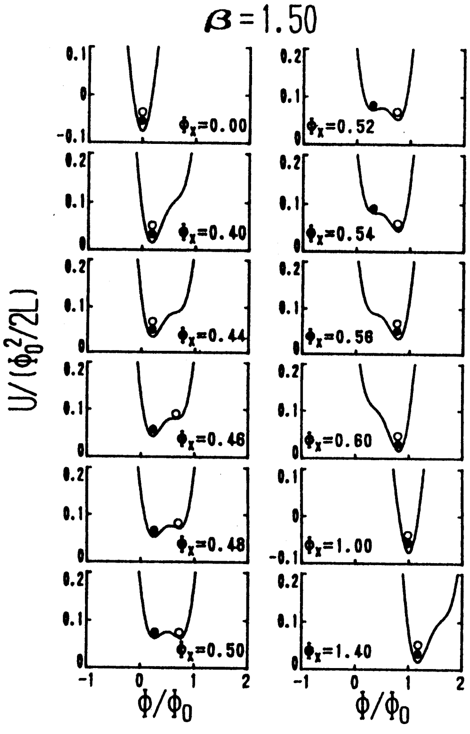

Fig. 9 Behavior of hysteresis in U for $\beta = 1.50$. With increasing external flux Φ_x the superconducting ring stays at the minimum point up to $\Phi_x / \Phi_0 = 0.500$. From 0.500 to 0.544 the system remains in the metastable state and the transition takes place at 0.544. On the other hand, with decreasing Φ_x the transition occurs at 0.456. For simple illustration, the solid circles indicate the flux in increasing process and the open circles show the flux in decreasing process.

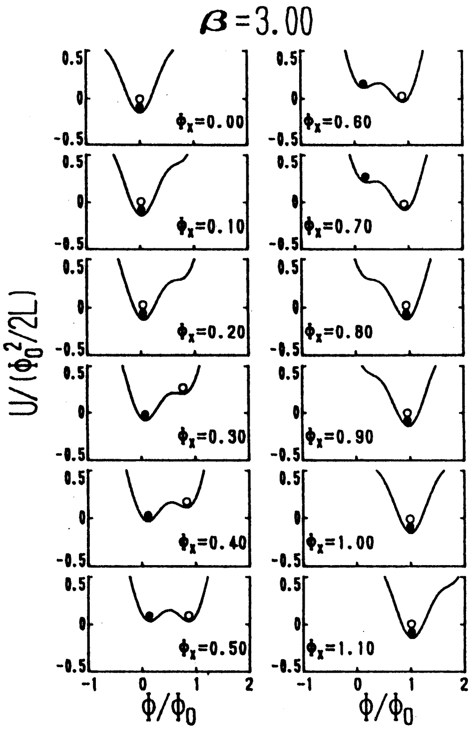

Fig. 10 Behavior of hysteresis in U for the case of $\beta = 3.00$. The hysteresis appears in the same way shown in Fig. 9. The value of Φ_x changes from 0.0 to 1.10.

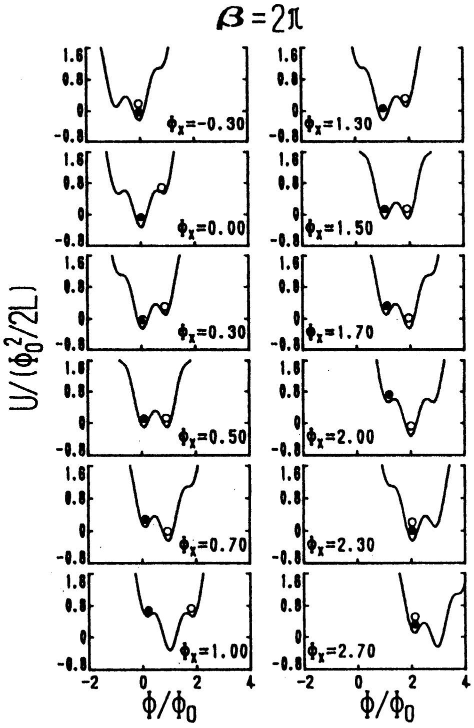

Fig. 11 Behavior of hysteresis in U for the case of $\beta = 2\pi$. The hysteresis appears in the same way shown in Fig. 9. The value of Φ_x changes from -0.30 to 2.70.

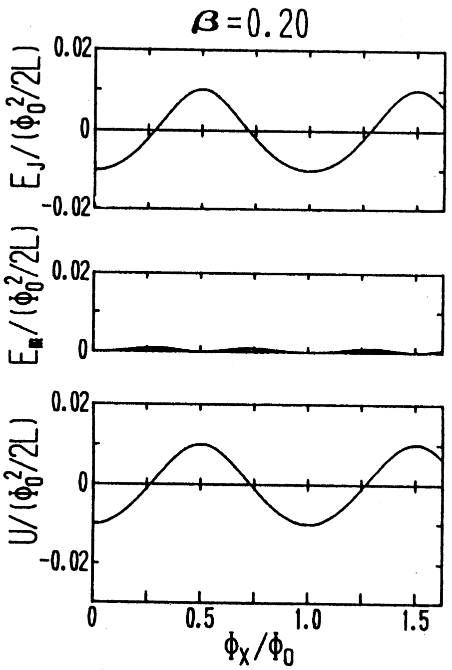

Fig. 12 Junction coupling energy E_J, magnetic energy E_m and system energy U as a function of the external flux Φ_x for $\beta = 0.20$. The value of U corresponds to the minimum value in Fig. 6.

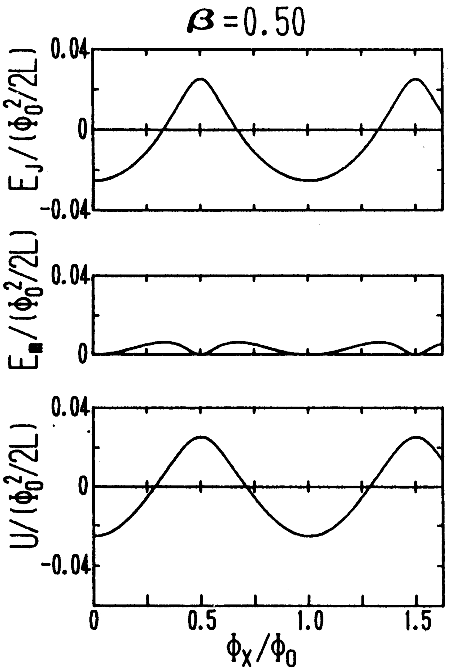

Fig. 13 E_J, E_m and U as a function of Φ_x for $\beta = 0.50$. The value of U corresponds to the minimum value in Fig. 7.

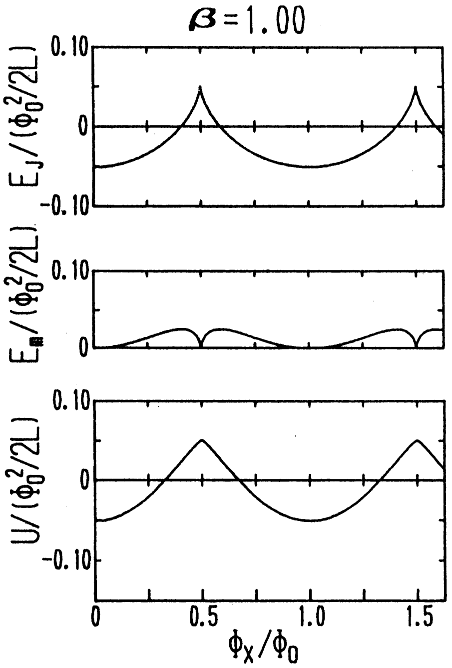

Fig. 14 E_J, E_m and U as a function of Φ_x for $\beta = 1.00$. The value of U corresponds to the minimum value in Fig. 8.

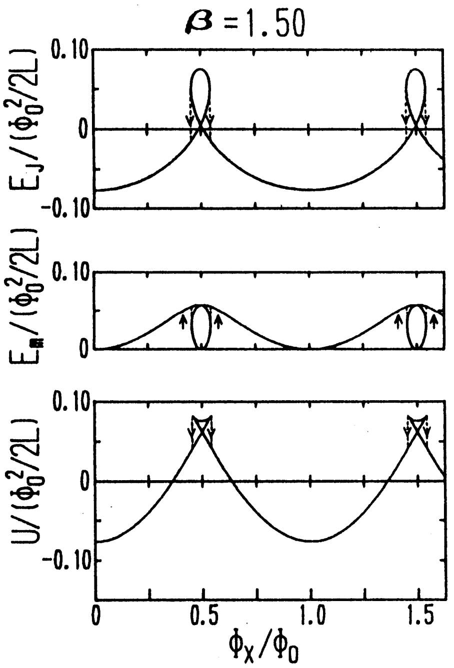

Fig. 15 E_J, E_m and U as a function of Φ_x for $\beta = 1.50$. The hysteresis with transitions at different Φ_x is indicated by arrows. The hysteresis behavior can be understood by considering the correspondence between Fig. 9 and Fig. 15. The value of U corresponds to the minimum or maximum value in Fig. 9.

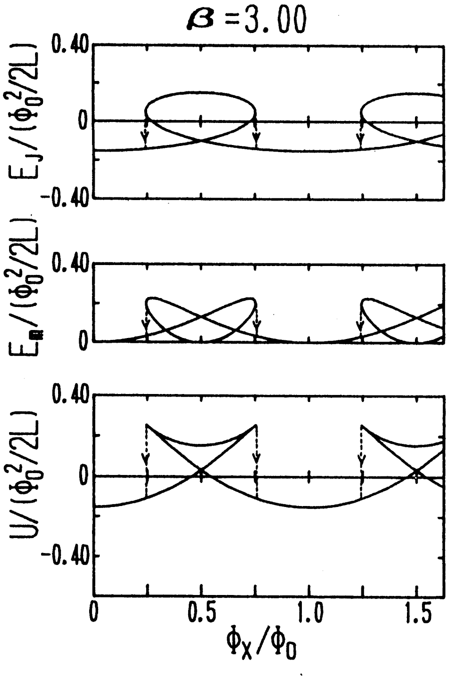

Fig. 16 E_J, E_m and U as a function of Φ_x for $\beta = 3.00$. The hysteresis behavior can be understood by considering the correspondence between Fig. 10 and Fig. 16. The value of U corresponds to the minimum or maximum value in Fig. 10.

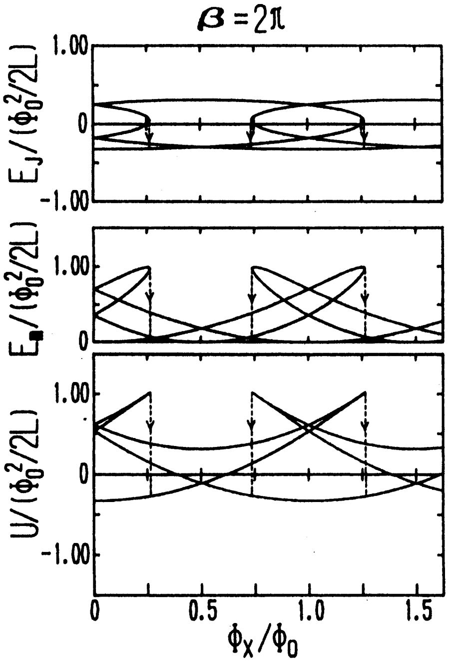

Fig. 17 E_J, E_m and U as a function of Φ_x for $\beta = 2\pi$. The hysteresis behavior can be understood by considering the correspondence between Fig. 11 and Fig. 17. The value of U corresponds to the minimum or maximum value in Fig. 11.

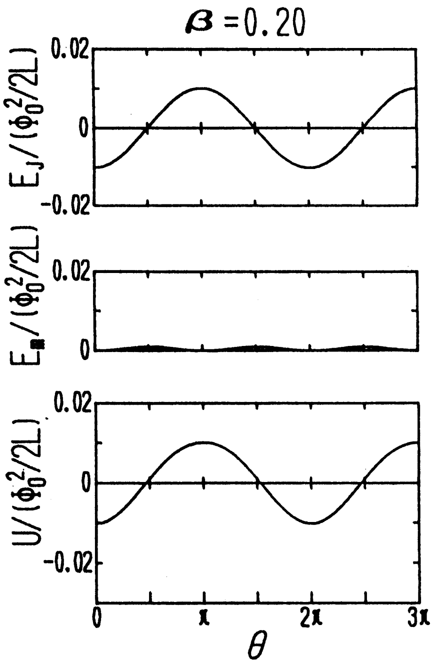

Fig. 18 Junction coupling energy E_J, magnetic energy E_m and system energy U as a function of the phase difference θ across the junction for $\beta = 0.20$.

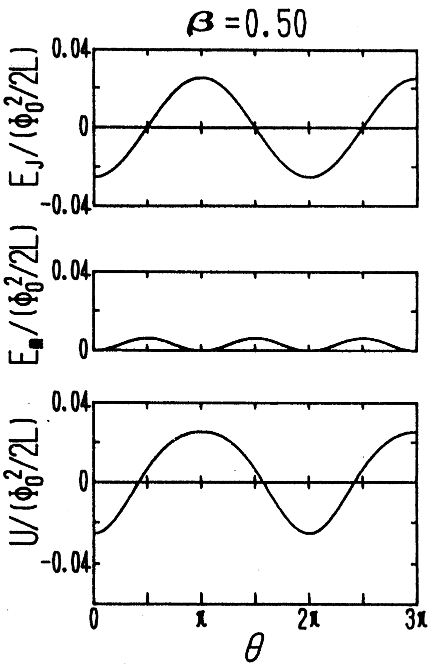

Fig. 19 E_J, E_m and system energy U as a function of θ for $\beta = 0.50$.

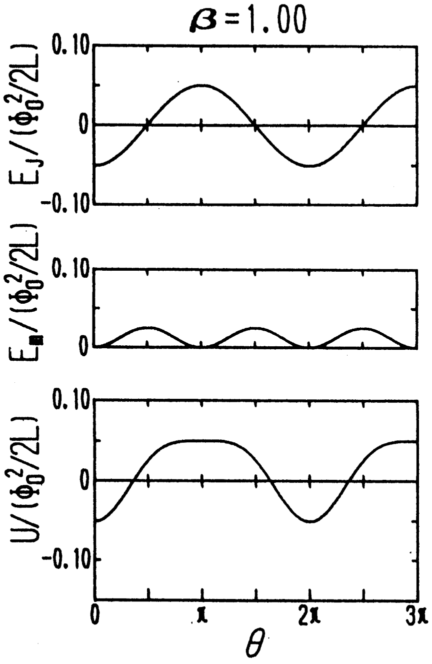

Fig. 20 E_J, E_m and system energy U as a function of θ for $\beta = 1.00$.

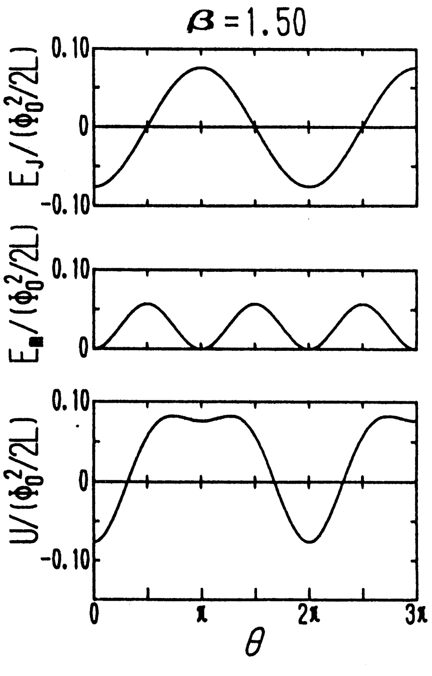

Fig. 21 E_J, E_m and system energy U as a function of θ for $\beta = 1.50$.

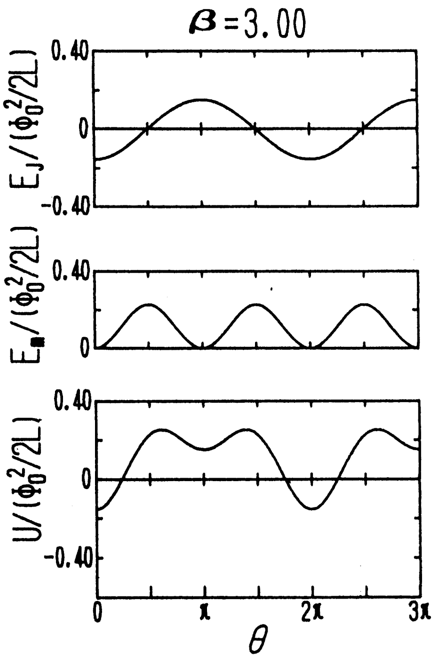

Fig. 22 E_J, E_m and system energy U as a function of θ for $\beta = 3.00$.

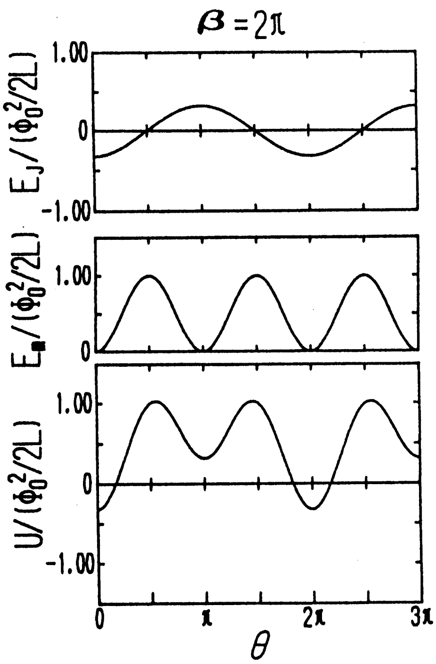

Fig. 23 E_J, E_m and system energy U as a function of θ for $\beta = 2\pi$.

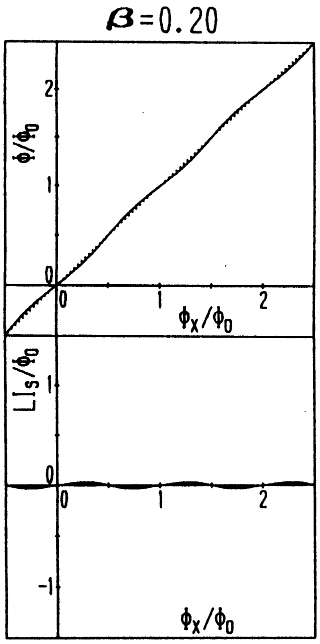

Fig. 24 Internal flux Φ and the flux LI_s induced by screening current as a function of the external flux Φ_x for $\beta=0.20$.

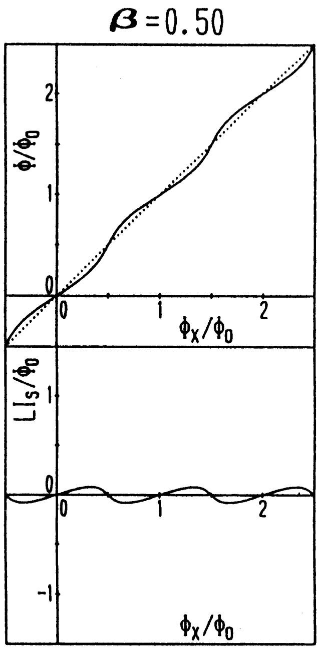

Fig. 25 Internal flux Φ and the induced flux LI_s as a function of Φ_x for $\beta = 0.50$.

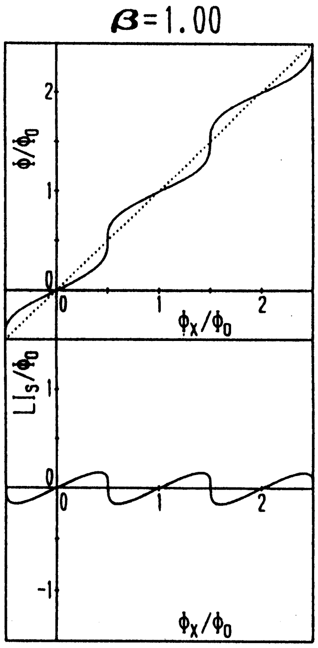

Fig. 26 Internal flux Φ and the induced flux LI_s as a function of Φ_x for $\beta = 1.00$.

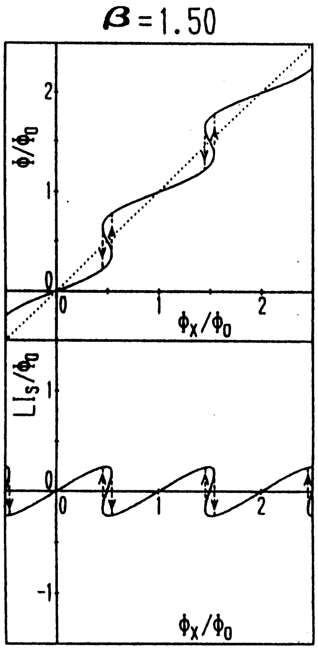

Fig. 27 Internal flux Φ and the induced flux LI_s as a function of Φ_x for $\beta = 1.50$. The hysteresis with transitions at different Φ_x is indicated by arrows. The hysteresis behavior corresponds to that in Fig. 9.

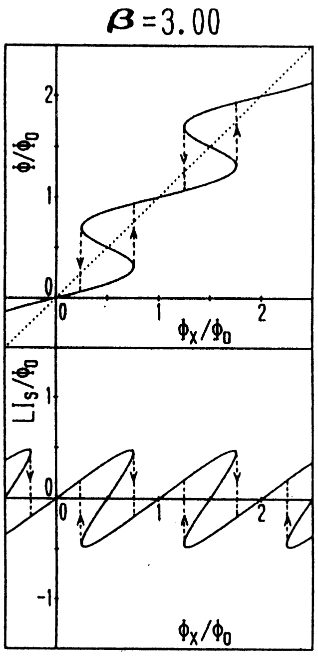

Fig. 28 Internal flux Φ and the induced flux LI_s as a function of Φ_x for $\beta = 3.00$. The hysteresis behavior corresponds to that in Fig. 10.

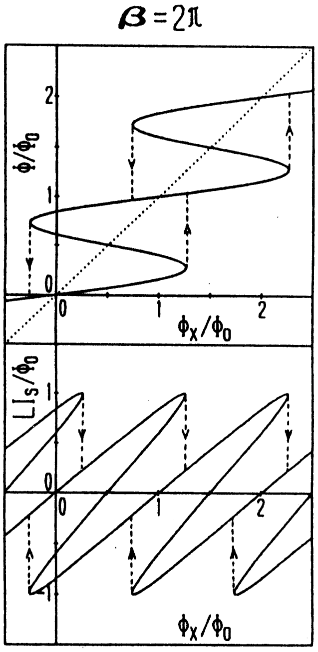

Fig. 29 Internal flux Φ and the induced flux LI_s as a function of Φ_x for $\beta = 2\pi$. The hysteresis behavior corresponds to that in Fig. 11.

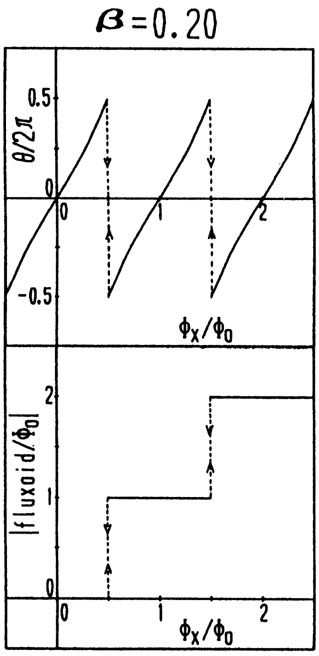

Fig. 30 Phase difference θ across the junction and fluxoid as a function of the external flux Φ_x for $\beta = 0.20$.

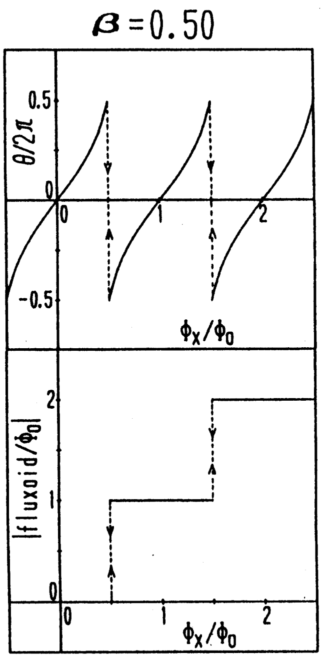

Fig. 31 Phase difference θ and fluxoid as a function of Φ_x for $\beta = 0.50$.

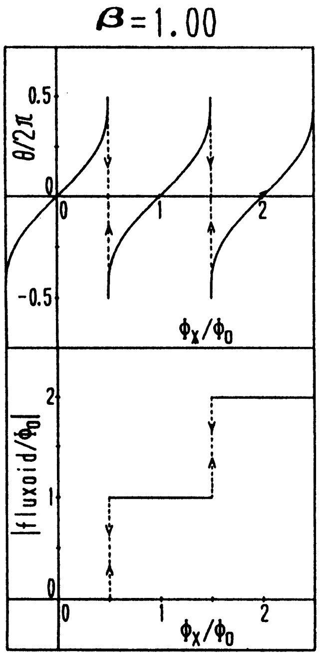

Fig. 32 Phase difference θ and fluxoid as a function of Φ_x for $\beta = 1.00$.

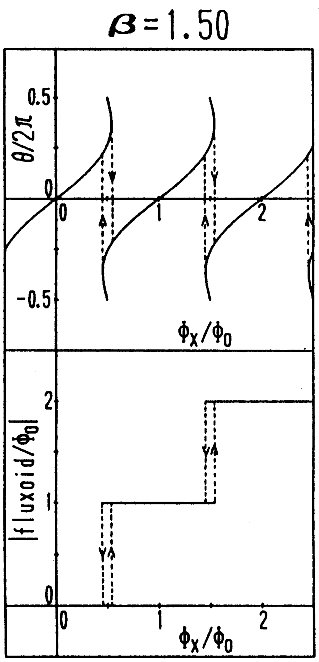

Fig. 33 Phase difference θ and fluxoid as a function of Φ_x for $\beta = 1.50$. The hysteresis with transitions at different Φ_x is indicated by arrows. The hysteresis feature corresponds to that in Fig. 9.

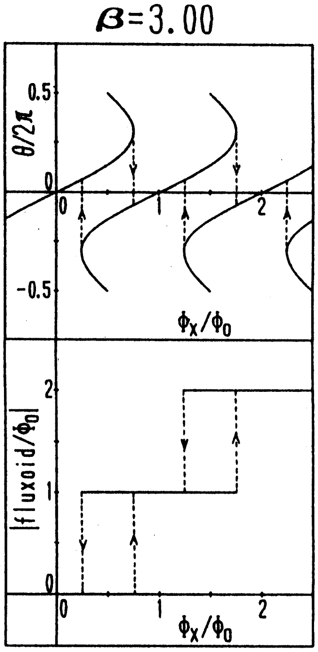

Fig. 34 Phase difference θ and fluxoid as a function of Φ_x for $\beta = 3.00$. The hysteresis feature corresponds to that in Fig. 10.

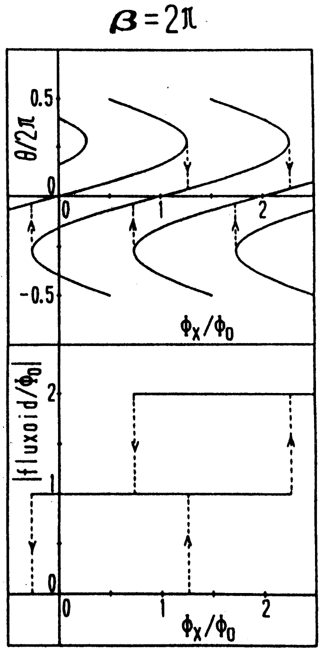

Fig. 35 Phase difference θ and fluxoid as a function of Φ_x for $\beta = 2\pi$. The hysteresis feature corresponds to that in Fig. 11.